


Parental centrioles are dispensable for deuterosome formation and function during basal body amplification

Huijie Zhao^{1,†}, Qingxia Chen^{2,†}, Chuyu Fang¹, Qiongping Huang¹, Jun Zhou³, Xiumin Yan^{1,*} & Xueliang Zhu^{1,2,**} 

Abstract

Mammalian epithelial cells use a pair of parental centrioles and numerous deuterosomes as platforms for efficient basal body production during multiciliogenesis. How deuterosomes form and function, however, remain controversial. They are proposed to arise either spontaneously for massive *de novo* centriole biogenesis or in a daughter centriole-dependent manner as shuttles to carry away procentrioles assembled at the centriole. Here, we show that both parental centrioles are dispensable for deuterosome formation. In both mouse tracheal epithelial and ependymal cells (mTECs and mEPCs), discrete deuterosomes in the cytoplasm are initially procentriole-free. They emerge at widely dispersed positions in the cytoplasm and then enlarge, concomitant with their increased ability to form procentrioles. More importantly, deuterosomes still form efficiently in mEPCs whose daughter centriole or even both parental centrioles are eliminated through shRNA-mediated depletion or drug inhibition of Plk4, a kinase essential to centriole biogenesis in both cycling cells and multiciliated cells. Therefore, deuterosomes can be assembled autonomously to mediate *de novo* centriole amplification in multiciliated cells.

Keywords basal body; centriole; deuterosome; multicilia; Plk4

Subject Categories Cell Adhesion, Polarity & Cytoskeleton; Cell Cycle

DOI 10.15252/embr.201846735 | Received 13 July 2018 | Revised 28 January 2019 | Accepted 6 February 2019 | Published online 4 March 2019

EMBO Reports (2019) 20: e46735

Introduction

Centriole biogenesis in cycling cells is tightly controlled [1–4]. In G1 phase of the cell cycle, each cell contains a centrosome with a pair of parental centrioles: the mother and daughter centrioles. In S

phase, the daughter centriole matures into a mother centriole. Both the older and younger mother centrioles are then allowed to assemble one nascent daughter centriole from a Cep63- and Cep152-containing platform [5,6], located around their basolateral walls, by restricting the levels and location of a critical protein kinase Plk4 [7–10]. Plk4 recruits and phosphorylates Stil, which then recruits SAS6 to initiate centriole biogenesis [4,11–13]. The SAS6-containing cartwheel further primes the assembly of other components such as the centriolar microtubules and Centrin into a procentriole [7,14–19]. In G2 phase, the daughter centriole assembly is complete. Following mitosis, the two pairs of mother–daughter centrioles are partitioned in the form of the centrosome into two progeny cells so that constant centriole number can be maintained [3,20]. Overexpressing key regulators such as Plk4, Cep152, and SAS6 have been shown to potentiate the centriole biogenesis ability of the parental centrioles [7,11,21–23].

Epithelial tissues such as those in mammalian trachea, ependyma, and oviduct are abundant in terminally differentiated cells with dense motile cilia. These multiciliated cells each require up to hundreds of centrioles to serve as basal bodies of their cilia [24–26]. To achieve this, the cells express high levels of proteins important for the massive basal body production through transcriptional regulators such as multicilin and E2f4 [27–32]. As a result, both parental centrioles produce multiple daughter centrioles. Furthermore, dozens of spherical structures termed deuterosomes emerge to generate the majority of the basal bodies [33–35]. The deuterosome adapts Deup1, a paralog of Cep63, and Ccdc78 to create a similar but parental centriole-free platform of centriole biogenesis [27,36–38]. Its formation requires cytoplasmic E2f4 [32]. Fully assembled centrioles are eventually released from their “cradles” by APC/C-activated proteolysis and mature into basal bodies [39,40].

The origin and functions of deuterosomes, however, are still controversial. Based mainly on electron microscopic studies, deuterosomes have been proposed to either form autonomously and

1 State Key Laboratory of Cell Biology, CAS Center for Excellence in Molecular Cell Science, Shanghai Institute of Biochemistry and Cell Biology, Chinese Academy of Sciences, University of Chinese Academy of Sciences, Shanghai, China

2 School of Life Science and Technology, ShanghaiTech University, Shanghai, China

3 Key Laboratory of Animal Resistance Biology of Shandong Province, Institute of Biomedical Sciences, College of Life Sciences, Collaborative Innovation Center of Cell Biology in Universities of Shandong, Shandong Normal University, Jinan, Shandong, China

*Corresponding author. Tel: +86 21 54921406; Fax: +86 21 54921011; E-mail: yanx@sibcb.ac.cn

**Corresponding author. Tel: +86 21 54921406; Fax: +86 21 54921011; E-mail: xlzhu@sibcb.ac.cn

†These authors contributed equally to this work

mediate parental centriole-independent, or *de novo*, centriole biogenesis [3,33,34,41] or form and support procentriole biogenesis in a parental centriole-dependent manner [42]. Our recent identification of Deup1 enables further examinations of these hypotheses using fluorescent microscopy. Our results in cultured mTECs strengthen the first model because deuterosomes are found to emerge massively, initially carrying fewer procentrioles (Fig 1A, stage II), and then grow into larger ones with more associated procentrioles (Fig 1A, stage III) [36]. A later study mainly using cultured mEPCs, on the other hand, elaborates the second model by proposing that all the deuterosome and procentrioles are initially nucleated from the daughter centrosomal centriole. Deuterosomes only function as shuttles to load and carry away these procentrioles in the form of “halos” to facilitate centriole amplification (Fig 1B) [43,44].

In this study, we sought to clarify the discrepancies using cultured mTECs and mEPCs.

Results and Discussion

Discrete deuterosomes in mTECs do not initially exist as halos

The global increase in the number of deuterosome-associated procentrioles from stage II to stage III in mTECs [36] clearly argues against the mere “shuttle” role of the deuterosome. Nevertheless, the initial procentrioles on the stage-II deuterosomes could still come from the centrosomal daughter centriole. To clarify this, we examined early events of deuterosome and procentriole formation. mTECs can be induced to differentiate into multiciliated cells efficiently by culturing at an air–liquid interface (ALI) [36,45,46]. As mTECs thus cultured for 3 days were mainly at late stages of the basal body production [36], we examined those at day 2 with three-dimensional structured illumination microscopy (3D-SIM).

Consistent with our previous report [36], both parental centrioles carried procentrioles in stage-II mTECs when they were both detected (Fig 1C and D). By contrast, the size and number of the deuterosomes and the status of their procentrioles, which were better defined by using both Sas6 and Centrin as markers (Fig 1D) [47,48], varied dramatically. For instance, a portion of the cells contained sparse, small ($\phi = 210 \pm 60$ nm), and usually procentriole-free deuterosomes (Fig 1C–E: IIa), suggesting that they are in early stage II (Fig 1F: IIa). In the remaining stage-II cells, deuterosomes were generally larger ($\phi = 280 \pm 50$ nm; Fig 1E: IIb/c) and more abundant (Fig 1C and D: IIb and IIc). Those mingled with deuterosomes either without procentriole or with only one procentriole were presumably in middle stage II (Fig 1C, D, and F: IIb). Sometimes, deuterosomes of both small and large sizes were observed in these cells (Fig 1D: IIb). By contrast, those with deuterosomes that were commonly associated with 1–2 procentrioles were in late stage II (Fig 1C, D, and F: IIc). In comparison, in stage-III mTECs deuterosomes were 340 ± 50 nm in diameter (Fig 1E) and frequently associated with 3–5 procentrioles (Fig 1C and F). Therefore, in mTECs discrete deuterosomes do not initially carry procentrioles as indicated by Al Jord and colleagues [43]. Neither does the marked increase in their associated procentrioles during the progression from stage II to stage III (Fig 1C) [36] fit the proposed shuttle function of the deuterosome (Fig 1B) [43].

Murine Ccdc78, whose *Xenopus* orthologue is identified as a deuterosome protein [38], was also used by Al Jord and colleagues as a deuterosome marker in addition to Deup1 [43]. We thus examined its subcellular localization but were unable to detect deuterosome localization of endogenous or exogenous murine Ccdc78 in mTECs. Both endogenous Ccdc78 and exogenous GFP-Ccdc78 formed numerous puncta irrelevant to deuterosomes in stages II–IV (Fig EV1A and B). In stage VI, they both showed correlation with basal bodies (Fig EV1A and B). As exogenous Deup1 can induce deuterosome-like structures in cycling cells [36], we co-expressed Flag-Deup1 and GFP-Ccdc78 in U2OS cells and still found no GFP-Ccdc78 on the deuterosome-like structures in the human cells (Fig EV1C). Instead, GFP-Ccdc78 mostly decorated a parental centriole (Fig EV1C). We have previously shown that in differentiating mTECs, the expression patterns of proteins involved in centriole amplification, such as Deup1, Plk4, Cep152, and Sas6, are similar, but distinct from those involved in ciliary biogenesis or functions, such as Odf2 and Ift57 [36]. Ccdc78, however, was different from Deup1 in expression patterns but analogous to centriolar appendage proteins Odf2 and Cep164 and ciliary protein Ift81 (Fig EV1D) [25,49,50]. These results do not suggest mammalian Ccdc78 as a deuterosome protein. We therefore only used Deup1 and Cep152 as deuterosome markers in the following experiments.

Centriole amplification in mEPCs resembles mTECs

Next, we investigated whether the centriole amplification process in mEPCs is different. Cultured progenitor cells isolated from P0 mouse brain tissues can be induced to differentiate into multiciliated mEPCs through serum starvation [51,52]. We examined the mEPCs at day 2 or 3 postserum starvation because they were undergoing active centriole amplification [43,53]. As Centrin-positive aggregates were frequently observed in mEPCs, especially in the area around the parental centrioles [54,55], we also used Sas6 as additional procentriole marker [47,48].

We found that mEPCs could also be grouped into six stages (Fig 2A and B), similar to mTECs (Fig 1A) [36]: (i) Those containing only a pair of Cep152-positive, Deup1-negative parental centrioles were in stage I; (ii) those containing small deuterosomes with mostly 0–2 procentrioles were in stage II; (iii) those in the “halo” or “flower” stages (see Fig 1B) [43], containing larger deuterosomes commonly with 3–7 procentrioles, could be assigned to stages III and IV, respectively. The stage-IV cells were also distinguished from those in stage III by the emergence of multiple Cep152-positive protrusions from both deuterosomes and parental centrioles. Their Centrin staining was also elongated as compared to the punctate staining in the stage-III cells; (iv) those with partially released basal bodies from their cradles were in stage V. Their basal bodies still contained the Sas6-positive puncta; and (v) those with fully released basal bodies negative for the Sas6 staining were in stage VI (Fig 2A and B). Similar to mTECs [36,53], stage-VI mEPCs also underwent multiciliogenesis (Fig 2C). Only their basal bodies did not group into clusters (Fig 2A–C) as those do in mTECs [36].

Quantifications indicated that $44.3 \pm 3.5\%$ (day 2) and $45.3 \pm 3.9\%$ (day 3) of the cells were morphologically in stage I (Fig 2D). In addition to those that would soon undergo deuterosome

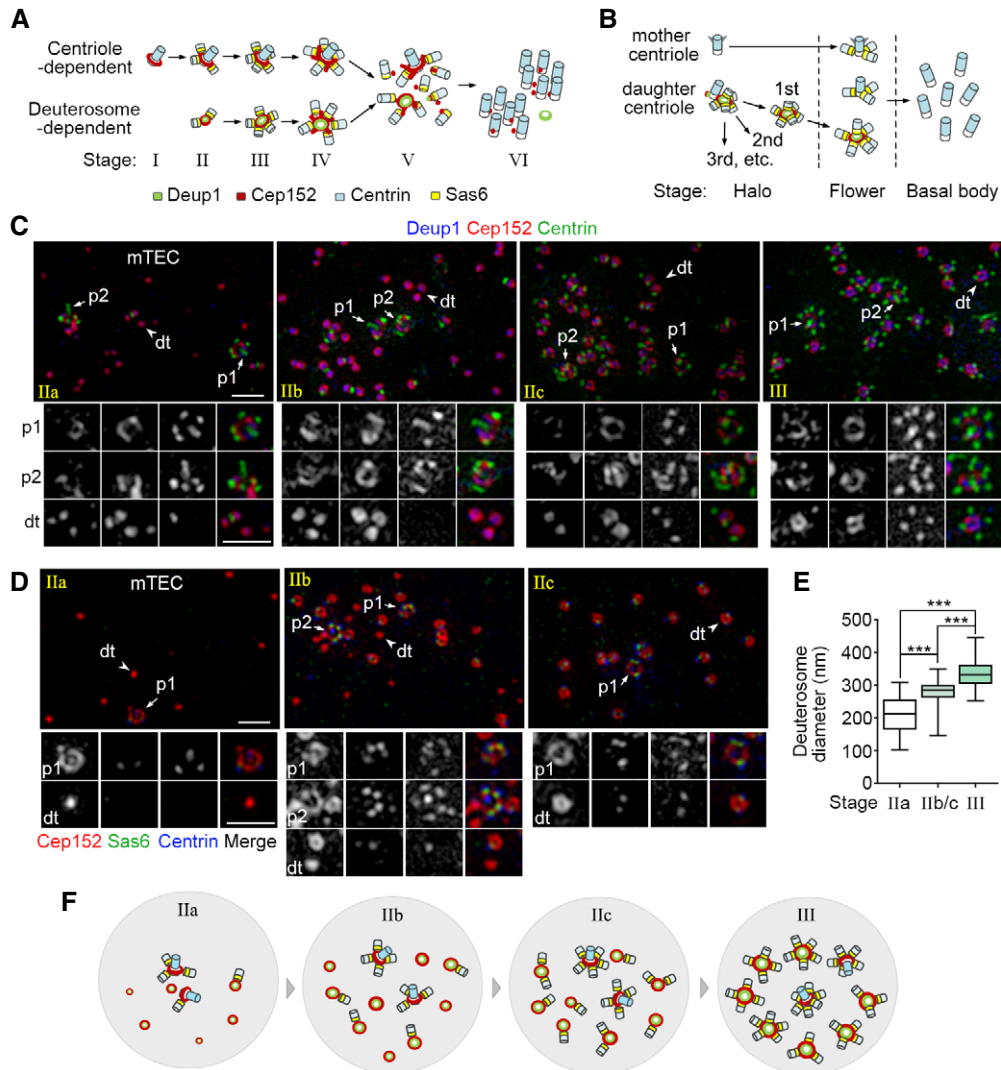


Figure 1. Discrete deuterosomes in mTECs are initially free of procentrioles.

A, B Two current models for the process of massive basal body formation based on studies in mTECs (A) and mEPCs (B). In (A), deuterosomes are proposed to form spontaneously in stage II and each supports the assembly of 1–2 procentrioles. They grow in size and nucleate more procentrioles in stage III. Each parental centriole also nucleates multiple procentrioles from stage II. Stage IV is characterized by the emergence of Cep152-positive protrusions, stage V by the releasing of basal bodies from both deuterosomes and parental centrioles, and stage VI by the formation of basal body clusters under the apical side of the cell membrane [36]. In (B), deuterosomes are assembled at the lateral wall of the daughter centriole and released one by one as procentriole-occupied “halos” (the halo stage). During this stage, parental centrioles also start to generate their own procentrioles. When the last halo is released, procentrioles on both deuterosomes and parental centrioles start to mature simultaneously (the flower stage) and are eventually released as basal bodies (the basal body stage) [43]. Deup1, Cep152, Centrin, and Sas6 are used as markers respectively for the deuterosome, both parental centriole and deuterosome, centriole (including procentriole), and procentriole.

C, D Representative mTECs containing early deuterosomes. mTECs cultured at an air–liquid interface for 2 days were immunostained for Cep152, Centrin, and Deup1 (C) or Sas6 (D) and subjected to 3D-SIM. Parental centrioles (p1/p2; arrows) and typical deuterosomes (dt; arrowheads) are magnified 1.5× to show details. IIa: Parental centrioles contain procentrioles; most deuterosomes are procentriole-free and usually small. IIb: A substantial portion of deuterosomes contains 1 procentriole; deuterosomes are usually medium in size. IIc: Most deuterosomes contain 1–2 procentrioles; deuterosomes are usually medium in size. A stage-III cell, which contained larger deuterosomes associated with more procentrioles, is shown in (C) for comparison. Scale bar, 1 μm.

E Deuterosome-size distributions in stage IIa, IIb/c, and III. For each group, the diameters of at least 348 deuterosomes were measured from 12 mTECs selected from three independent experiments according to the stages. The bottom and top of the box represent the 25th and 75th percentiles, respectively. The band is the median. The ends of the whiskers indicate the maximum and minimum of the data. Two-tailed unpaired Student’s t-test: ****P* < 0.001.

F An illustration model for the progression of mTECs from stage IIa to III.

formation, this population also contained cells of other fates because 30–60% of mEPCs were multiciliated at day 5 or later [51–53]. The mEPCs at early stages were more abundant at day 2 than day 3. For instance, stage-II cells occupied $41.3 \pm 2.7\%$ at day 2 but $23.8 \pm 5.0\%$ at day 3 (Fig 2D). On the other hand, 17.4% of the

mEPCs were in stages IV–VI at day 3, whereas at day 2 only 4.1% of the cells were in stages IV–V and no stage-VI cells were observed (Fig 2D). These results further support the conclusion that mEPCs progress from stage I to VI during their differentiation into multiciliated cells.

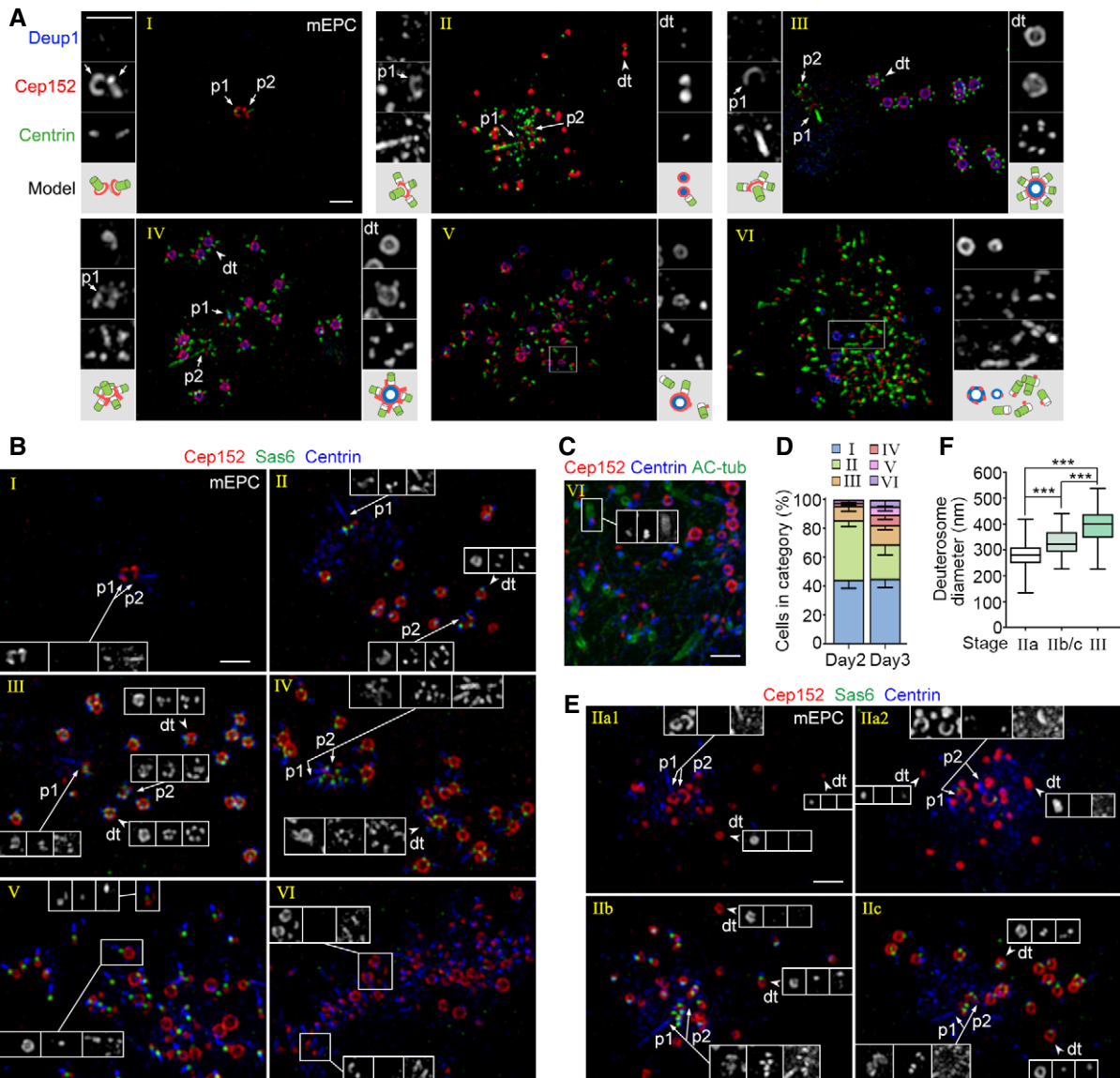


Figure 2. mEPCs resemble mTECs in centriole amplification.

- A Typical mEPCs representing different stages of centriole amplification. mEPCs cultured under serum starvation for 3 days were immunostained for Deup1, Cep152, and Centrin, followed by imaging with 3D-SIM. Parental centrioles (p1/p2; arrows), typical deuterosomes (dt; arrowheads), and typical regions with basal bodies (framed) are magnified 2 \times to show details. An illustration is provided for each set of the magnified images. Scale bar, 1 μ m.
- B Typical mEPCs at day 3, immunostained for Cep152, Sas6, and Centrin. The insets are arranged in the same sequence from left to right. Scale bar, 1 μ m.
- C Multicilia formation in a typical stage-VI mEPC. Acetylated tubulin (AC-tub) was used as ciliary marker. Note that the ciliogenesis is asynchronous. Scale bar, 1 μ m.
- D Stage distributions of mEPCs at day 2 and 3. The histograms represent mean values from three independent experiments. At least 108 cells were scored in each experiment and condition. Error bars represent SD.
- E Discrete deuterosomes in early stage-II mEPCs were also procentriole-free. mEPCs at day 2 were immunostained for Cep152, Sas6, and Centrin. The insets are arranged in the same sequence from left to right. Scale bar, 1 μ m.
- F Deuterosome-size distributions. For each group, the diameters of at least 496 deuterosomes were measured from 32 mEPCs selected from three independent experiments according to the stages. The bottom and top of the box represent the 25th and 75th percentiles, respectively. The band is the median. The ends of the whiskers indicate the maximum and minimum of the data. Two-tailed unpaired Student's *t*-test: ****P* < 0.001.

For further clues on early phases of the deuterosome formation, we examined the stage-II mEPCs in detail. We found that, similar to mTECs (Fig 1), stage-II mEPCs could also be grouped into those in IIa, IIb, and IIc (Fig 2E). The average deuterosome diameters were 280 ± 60 nm (IIa) and 330 ± 60 nm (IIb/c), which were smaller than those in stage-III mEPCs (390 ± 80 nm; Fig 2F).

Furthermore, when both parental centrioles were detected in the mEPCs at stage IIb or IIc, they all bore procentrioles (Fig 2E; also see Fig 2A and B). This was also true for the cells in stage III or IV (Fig 2A and B). In the stage-IIa mEPCs, however, parental centrioles that were with or without procentrioles were observed (Fig 2E: IIa1 and IIa2). Therefore, even in mEPCs discrete

deuterosomes do not initially exist as “halos” as reported (Fig 1B) [43], which makes it difficult to attribute all the procentrioles in the halos to the daughter centriole.

Nascent deuterosomes emerge from a wide variety of locations in mEPCs

To clarify the origin of the deuterosomes, we performed live cell imaging by using GFP-Deup1 to directly label deuterosomes [36]. To mimic the transient expression pattern of endogenous Deup1 [36], we cloned the mouse *Deup1* promoter and used it to drive *GFP-Deup1* expression (Fig 3A). We confirmed that GFP-Deup1 was specifically expressed together with endogenous Deup1 and Plk4 in

differentiating mEPCs at day 3, but not in the progenitor cells (Fig 3B and C). Its levels were low as compared to endogenous Deup1 (Fig 3C) and would thus minimize possible side effects of overexpression. 3D-SIM also confirmed its specific expression in the cells undergoing centriole amplification and proper localization at the center of deuterosomes (Fig 3D).

We imaged the differentiating mEPCs for deuterosome formation events with spinning disk microscopy at 5-min intervals for up to 12.5 h from day 2.5. We performed serial z-stack sectioning at 0.5- μ m intervals to cover a depth of 20 μ m and analyzed z-projections of the images. Initially, we found that GFP-positive puncta, presumably deuterosomes, moved rapidly and were difficult to trace over time (Movie EV1). Impairing microtubule-dependent intracellular

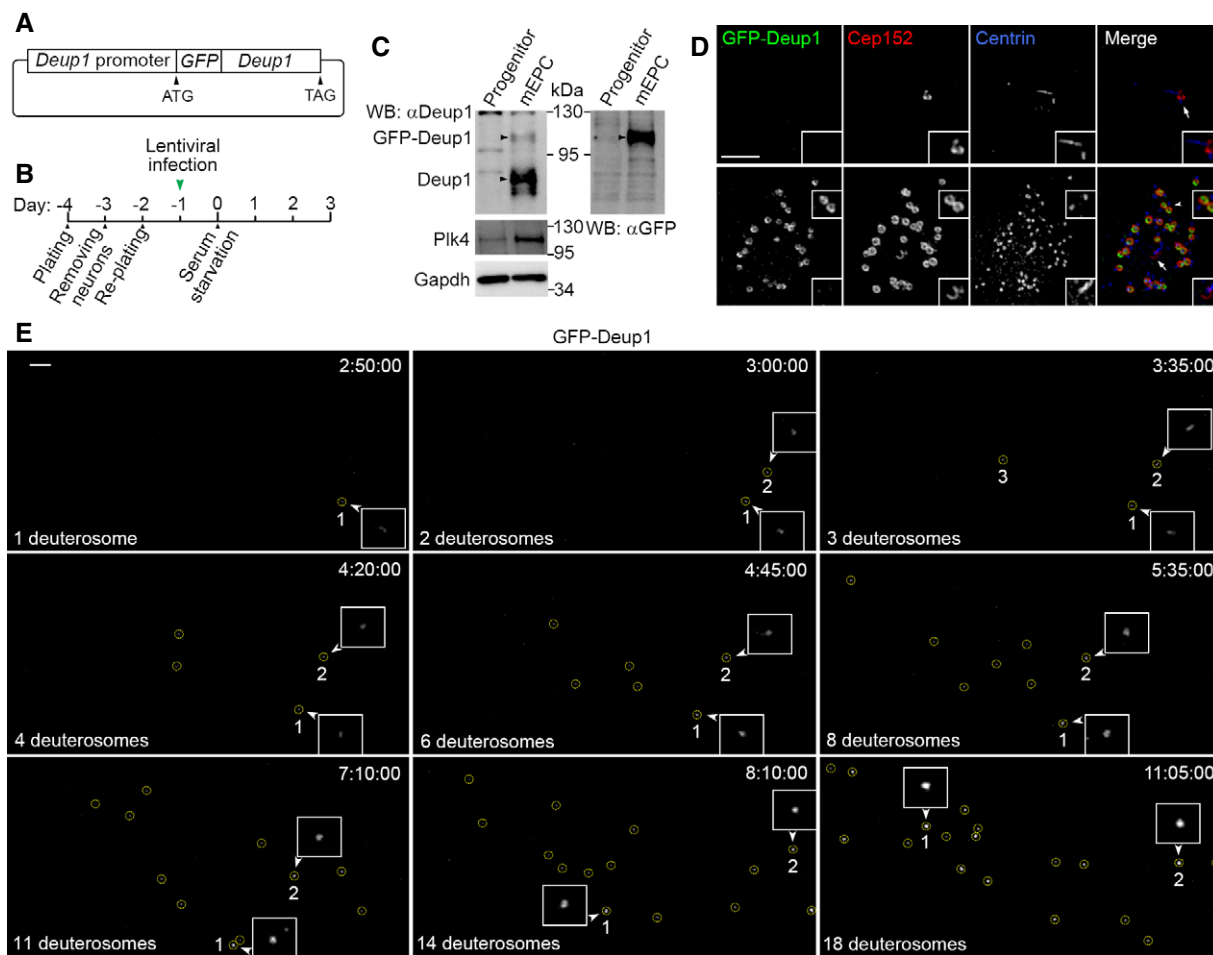


Figure 3. Deuterosomes emerge in a dispersed fashion in mEPCs.

A Schematic illustration of the lentiviral construct used in the experiment. A 2-kb mouse *Deup1* genomic DNA fragment upstream of the first exon was used as the *Deup1* promoter to drive the expression of *GFP-Deup1*.

B Experimental scheme. Progenitors of mEPCs isolated from P0 mouse brain tissues were cultured for 6 days and infected with lentivirus described in (A) for 24 h, followed by serum starvation (day 0) to induce differentiation.

C Specific expression of GFP-Deup1 in mEPCs. mEPCs treated as in (B) were collected at day 3 for immunoblotting to detect the indicated proteins (arrowheads). An aliquot of the infected progenitor cells was cultured to day 3 without serum starvation and used as control. Gapdh served as loading control.

D Specific expression and deuterosome localization of GFP-Deup1 in mEPCs undergoing centriole amplification. mEPCs treated as in (B) were fixed at day 3; immunostained to visualize GFP, Cep152, and Centrin; and imaged with SIM. The insets are magnified images (1.5 \times) for deuterosomes (arrowhead) and parental centriole (arrow). Note that the top cell was not undergoing centriole amplification. Scale bar, 2 μ m.

E Representative frames cropped from Movie EV2 to show the emergence of deuterosomes (encircled) in live imaging. Elapsed time is shown as h:mins. The first two deuterosomes are marked, because they were traceable, and magnified 2 \times to show details. Scale bar, 2 μ m.

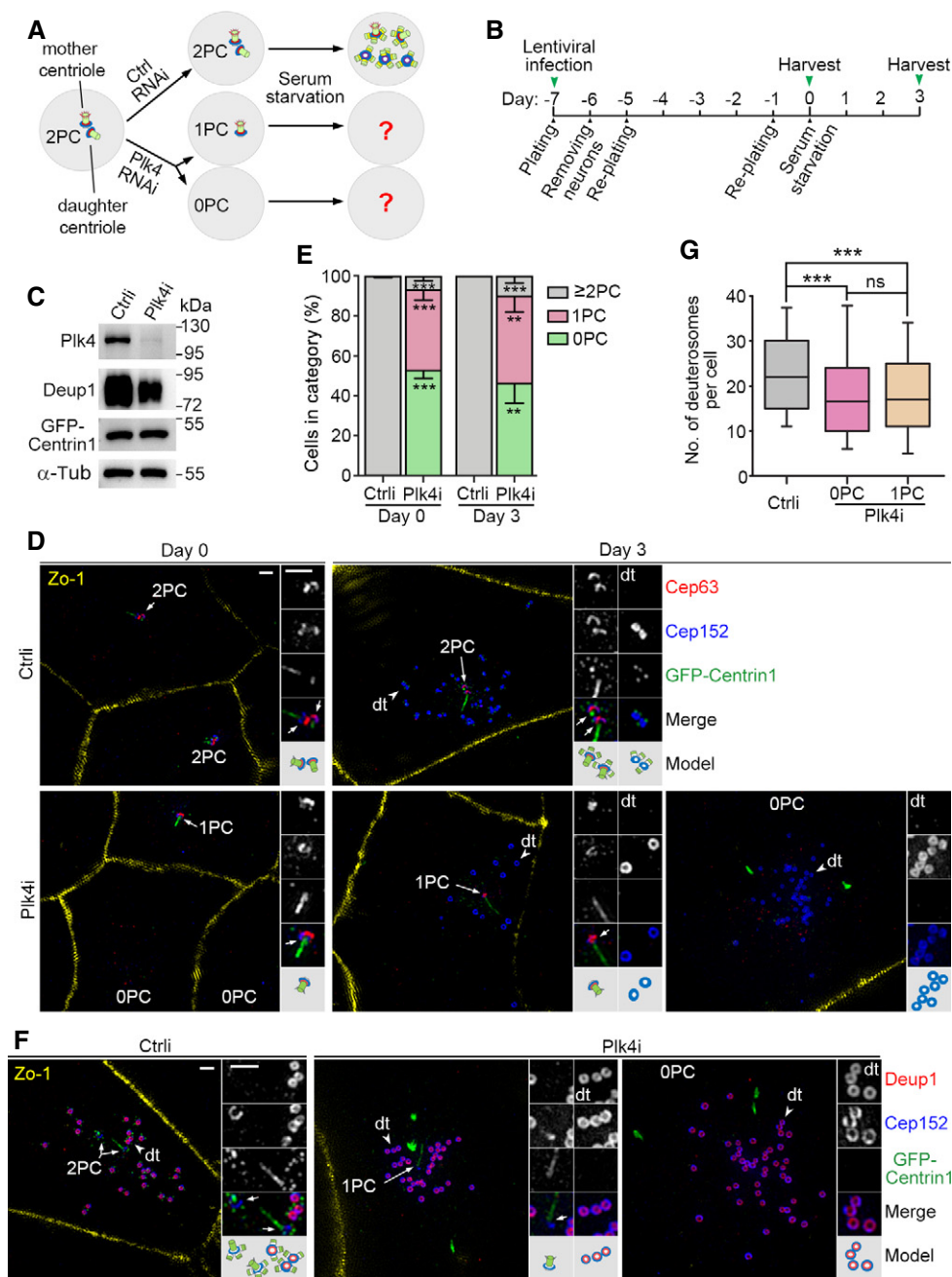


Figure 4.

transport [56] by treating the cells with nocodazole (0.5 $\mu\text{g}/\text{ml}$), a microtubule-destabilizing drug, markedly slowed down the deuterosome motilities. In the presence of nocodazole, we captured 15 cells that initiated their deuterosome biogenesis during the imaging (Fig 3E and Movie EV2) and 16 cells that already contained deuterosomes from the beginning and showed increased numbers of their deuterosomes over time (Movie EV3). Although clearly tracing every deuterosome was still difficult, the deuterosomes were found to initially emerge as tiny dim foci and enlarged dramatically over time with accordingly increased GFP-Deup1 fluorescent intensity (Fig 3E, and Movies EV2 and EV3). More importantly, nascent deuterosomes emerged at widely dispersed positions in these cells.

Multiple deuterosomes were observed to appear from different locations within minutes or an hour (Fig 3E, and Movies EV2 and EV3). These results are in sharp contrast to the observations by Al Jord and colleagues that deuterosomes require hours to form only at the daughter centriole and release from it [43]. Therefore, they strongly suggest that deuterosomes self-assemble efficiently.

Parental centrioles are dispensable for deuterosome formation

Next, we directly assessed the contribution of parental centrioles in deuterosome formation. We reasoned that, as Plk4 is essential for centriole biogenesis in both cycling and multiciliated cells [7–9,36],

Figure 4. Deuterosomes form efficiently in the absence of parental centrioles.

- A, B Experimental design. Depletion of Plk4 will abolish centriole biogenesis and result in loss of one (1PC) or both (0PC) of the two parental centrioles (2PC) during the proliferation of ependymal progenitor cells, which can then be used to examine how parental centrioles contribute to the deuterosome formation (A). We transfected the progenitors prepared from P0 mouse brain tissues with lentiviral particles at day -7 to silence Plk4 expression and examined their progeny cells at day 0 and 3 (B).
- C Confirmation of the Plk4 RNAi efficiency using mEPCs at day 3. The reduced expression of Deup1 in the Plk4-depleted cells is attributed to reduced multiciliate cell differentiation.
- D Typical cells immunostained for Zo-1, Cep152, and Cep63. GFP-Centrin1 expressed from the lentiviruses served as both infection and centriole markers. The green fluorescence was enhanced using anti-GFP antibody and Alexa Fluor-488-conjugated secondary antibody. Parental centrioles (arrows) and representative deuterosomes (dt; arrowheads) are magnified twofold to show details. An illustration is provided for each set of the magnified images. Parental centrioles were identified based on the co-staining patterns of Cep63, Cep152, and GFP-Centrin1. The strong GFP-Centrin1-positive streaks or speckles in the Plk4-depleted cells are not considered as centrioles because they did not co-stain with other centriolar markers. Scale bar, 1 μm .
- E Parental centriole contents of the cells. The histograms represent mean values from three independent experiments. At least 186 cells at days 0 and 80 and deuterosome-containing cells at day 3 were examined in each experiment and condition. Parental centrioles were identified based on the co-staining patterns of at least two different centriolar markers. Error bars represent SD. Two-tailed paired Student's *t*-test, $^{**}P < 0.01$; $^{***}P < 0.001$.
- F Confirmation of deuterosome formation in Plk4i-expressing mEPCs at day 3 by co-staining for Deup1 and Cep152. Parental centrioles (arrows) and representative deuterosomes (dt; arrowheads) are magnified twofold to show details. Scale bar, 1 μm .
- G Box plots for deuterosome numbers per cell. At least 156 deuterosome-containing cells from three independent experiments were examined. Deuterosomes were scored as ring-shaped structures decorated by both Deup1 and Cep152 (F) or by Cep152 but excluding parental centrioles (E). The bottom and top of the box represent the 25th and 75th percentiles, respectively. The band is the median. The ends of the whiskers indicate the 10th and 90th percentiles of the data. Two-tailed unpaired Student's *t*-test: ns, no significance; $^{***}P < 0.001$.

its depletion in proliferating ependymal progenitors would result in the cells with either one parental centriole or no parental centriole (Fig 4A). Inducing their differentiation by serum starvation would allow us to examine how the deuterosome formation is affected by parental centrioles (Fig 4A).

We have previously established a lentivirus that can stably co-express an infection marker GFP-Centrin1 with Plk4i, a short hairpin RNA (shRNA) against the murine Plk4 mRNA [36]. We found that infecting ependymal progenitors with the virus for 7 days before serum starvation efficiently depleted Plk4 (Fig 4B and C). When Zo-1, a tight junction protein [57], was used to mark cell boundaries, co-staining Cep152 with a parental centriole-specific marker, Cep63 [5,36,58], indeed revealed that an average of 40.2% or 53.0% of the ependymal progenitors respectively lost one parental centriole (1PC) or both parental centrioles (0PC) immediately before serum starvation (day 0; Fig 4D and E). In comparison, 99.8% of the cells infected with a lentivirus co-expressing a control shRNA (Ctrl) with GFP-Centrin1 contained two or more parental centrioles ($\geq 2\text{PC}$; Fig 4E).

Notably, 33.6% of the Plk4-depleted mEPCs at day 3 ($n = 113$ cells) were found to still contain deuterosomes (Fig 4D), which were further confirmed by co-staining with Deup1 (Fig 4F). In comparison, deuterosome-containing cells occupied 52.1% of the control virus-infected mEPCs at day 3 ($n = 71$ cells). As expected, procentriole formation was abolished in the Plk4-depleted mEPCs ($n = 100$ cells; Fig 4D and F). More importantly, 46.5% of the deuterosome-producing cells had no parental centriole, whereas 43.5% of them contained a single parental centriole (Fig 4D–F). Only a small portion (10.0%) contained two or more parental centrioles (Fig 4E). Quantifications revealed that deuterosome numbers in the mEPCs with no or one parental centriole were very similar (Fig 4G). The average numbers were 19.3 ± 13.2 ($n = 172$ cells) and 19.2 ± 12.4 ($n = 156$ cells), respectively. Deuterosome numbers increased slightly in the control mEPCs (Fig 4G), with an average of 23.8 ± 11.5 ($n = 316$ cells). These results indicate that parental centriole is not important for deuterosome formation. The reduced percentage of the deuterosome-containing Plk4-depleted cells at day 3 correlated with the reduced protein levels of Deup1 (Fig 4C), suggesting a decreased differentiation potency of the progenitors, possibly due to Plk4 depletion-induced self-renewal defects [59].

We also confirmed the parental centriole-independent deuterosome formation by using Cep164 and Odf2, which localize to centriolar appendages of the mother centriole [32,49,50] or Centrobilin, a daughter centriole-specific protein [60], as markers, together with Cep152 and GFP-Centrin1. In the control virus-infected progenitors immediately before serum starvation (day 0), both parental centrioles were positive for Cep152 but only one of them (the mother centriole) was positive for Cep164 and Odf2 (Fig 5A and B). By contrast, in the Plk4-depleted cells at day 0 or 3, when only one parental centriole was recognized, it was always double positive for Cep152-Cep164 or Cep152-Odf2, indicating that this centriole is the mother centriole (Fig 5A and B). Centrobilin staining revealed that mother centriole accounted for approximately 92% of the Plk4-depleted progenitors with one parental centriole at day 0 (Fig EV2A and B). At day 3, deuterosomes formed in the mEPCs with one or no recognizable parental centriole (Fig 5A and B).

Immunostaining using the ciliary marker acetylated tubulin [61] confirmed that a cilium ($1.2 \pm 0.5 \mu\text{m}$ in length; $n = 424$) already existed in the progenitors at day 0 (Figs 5C, and EV3A and B) as reported [51]. The cilium became elongated at day 3 ($3.9 \pm 1.4 \mu\text{m}$ in length; $n = 436$; Figs 5C, and EV3A and B). Interestingly, some of control virus-infected mEPCs at day 3 contained two cilia (Fig 5C). Consistently, in some of the stage-III control mEPCs, both parental centrioles were positive for Cep164 and Odf2 (Fig 5A and B), suggesting maturation of the daughter centriole into a basal body. This is interesting because in cycling cells the daughter centriole needs to go through mitosis to mature into the mother centriole, which possesses appendages and can serve as a basal body [2,15]. Possibly, this unexpected centriole maturation is rendered by the recently reported mitosis-like program in the differentiating mEPCs [39]. In addition, the bottom region of these cilia was usually Centrin-positive (Fig 5C) [43]. This explains the frequent observation of a Centrin-positive stick over the appendages of the mother centriole (Figs 2, 4, and 5), though its physiological significance remains to be clarified.

To further corroborate the parental centriole-independent deuterosome assembly, we treated ependymal progenitors with centrinone, a chemical inhibitor of Plk4 [62] (Fig EV4A). We tested different concentrations and found that 1.5 μM of centrinone

provided the best centriole depletion efficiency with low mortality in ependymal progenitors (Fig EV4B). At 3.0 μM concentration, cell death was prominent. We thus performed the subsequent experiments using 1.5 μM concentration. When the DMSO-treated cells were immunostained with Cep164, Cep152, and Centrin, they did not display centriole loss at both day 0 and 3 (Fig EV4C and D). By contrast, 51.6% of the centrinone-treated progenitors at day 0 contained no or one parental centriole (OPC + 1PC; $n = 488$ cells). At day 3, 65.7% of the deuterosome-containing cells treated with centrinone ($n = 134$ cells) contained no or one parental centriole (Fig EV4C and D). Quantification indicated that the deuterosome numbers in the cells with no parental centriole (34.2 ± 16.2 ; $n = 66$ cells) or one parental centriole (35 ± 12.9 ; $n = 31$ cells) were similar but increased as compared to the DMSO-treated cells (20.7 ± 11.1 ; $n = 102$ cells; Fig EV4E). The increase could be attributed to the limited sample size or other unknown effects of the drug. In addition, procentrioles were observed on deuterosomes in most centrinone-treated cells at day 3 (97%; $n = 97$ cells; Fig EV4D), possibly due to the failure of the centrinone to inhibit the markedly elevated levels of Plk4 in these cells (Fig 3C) [36]. Taken together, we demonstrate that parental centrioles are not important for deuterosome formation.

During the revision of the manuscript, two preprints posted online in bioRxiv also report similar parental centriole-independent deuterosome formation in centrinone-treated mTECs and mEPCs, respectively [preprint: 63, preprint: 64]. One of the preprints [preprint: 64] is posted by the same group that has previously proposed the daughter centriole-dependent model of deuterosome formation [43]. It is known that in cycling cells, centrioles can be assembled *de novo* in the absence of parental centrioles [65–68]. The presence of parental centriole inhibits the activation of the *de novo* pathway to avoid deregulated centriole formation [65]. Apparently, deuterosomes are able to efficiently form and fully function in the absence of parental centrioles. Moreover, our live imaging results (Fig 3; Movies EV2 and EV3) indicate that their spontaneous assembly is not repressed by parental centrioles.

The efficient, spontaneous formation of deuterosomes (Figs 3–5 and EV4, and Movies EV2 and EV3) [preprint: 63, preprint: 64] accordingly suggests that the daughter centriole does not possess a unique mechanism to induce deuterosome assembly as proposed [43,44]. Deup1 is sometimes observed to co-localize with Cep152 at both the mother and the daughter centrioles (Fig 1C) [27,36]. The parental centriole-localized Deup1 can even replace Cep63 to sustain the centriole-dependent procentriole assembly [36]. Deuterosomes may thus form from the centriolar Deup1, Cep152, Plk4, and other unknown proteins, if any, through mechanisms identical or similar to those that govern their autonomous assembly. Such deuterosomes keep associated with parental centrioles until they are released as halos [43]. Consistently, Mercey and colleagues also provide evidence in their preprint to suggest that the mother centriole is capable of deuterosome formation as well [preprint: 64].

The results to date also strengthen the idea that the deuterosome indeed functions as a platform for massive *de novo* procentriole biogenesis (Fig 1A) [27,36]. In centrinone-treated, parental centriole-ablated mEPCs, procentriole-associated deuterosomes were still observed (Fig EV4) [preprint: 64]. When centrinone was removed at day 0, the deuterosomes exhibit similar ability to associate with procentrioles as those in mEPCs with intact parental centrioles

[preprint: 64]. Nor are the total numbers of centrioles produced in the parental centriole-ablated mEPCs reduced as compared to the control cells [preprint: 64]. Similar situations occur in mTECs [preprint: 63]. Therefore, deuterosomes are still fully functional in procentriole biogenesis in the absence of parental centrioles.

Taken together, we propose that in differentiating multiciliated cells, deuterosomes form mainly in the cytosol and less frequently at the parental centrioles. Both the deuterosomes and the parental centrioles induce procentriole biogenesis to maximize the efficiency of the centriole amplification. Although multiple studies suggest that the centriole amplification processes are similar in multiciliated tissues and *in vitro* cultured multiciliated cells [43,45,46,69], future studies are still required to clarify whether deuterosomes are generated in the same way *in vivo*.

Materials and Methods

Cell culture, lentivirus production, and infection

mTECs were isolated from 4-week C57BL/6J mice and cultured as described previously [36]. mEPCs were cultured as described [51,52] with some modifications. Briefly, the telencephalon was dissected from P0 mice, followed by careful removal of the meninx, choroid plexus, hippocampus, and olfactory bulb in dissection buffer (161 mM NaCl, 5 mM KCl, 1 mM MgSO_4 , 3.7 mM CaCl_2 , 5 mM HEPES, and 5.5 mM glucose, pH 7.4) on ice. The remaining tissues were cut into small pieces and digested in freshly prepared digestion buffer (10 U/ml papain, 0.2 mg/ml L-cysteine, 0.5 mM EDTA, 1 mM CaCl_2 , 1.5 mM NaOH, and 5 U/ml DNase I in the dissection buffer) for 30 min at 37°C. The digestion was then stopped by adding 10% FBS. After gentle pipetting with a P1000 tip, the cells were collected by centrifugation at $400 \times g$ for 5 min at room temperature. The pelleted cells were re-suspended in the culture medium and seeded in a laminin-coated flask. Neurons were shaken off after a 1-day culture, and the remaining cells were further cultured to reach confluency. The cells were then transferred into the wells of laminin-coated 29-mm glass-bottomed dishes (Cellvis, D29-14-1.5-N) at a density of 2×10^5 cells per well and were maintained in serum-free medium to induce multiciliate mEPCs.

Lentiviral productions for the RNAi experiments were performed as described previously [36]. Eighteen 10-cm dishes of HEK293T cells transfected for 48 h were used to produce the lentiviral particles, which were further concentrated to 1 ml. Ependymal progenitor-enriched brain cells isolated from three P0 mice were re-suspended into 10 ml of the culture medium [51,52] containing 60 μl of the concentrated lentiviral particles and seeded into a 75- cm^2 flask (day –7). To suppress the p53-dependent apoptosis associated with centriole loss [70], 10 μM of the p53 inhibitor, pifithrin- α (S2929, Selleckchem), was always included in the culture medium to sustain cell viability [71]. After 24 h of culture, neurons were shaken off and fresh culture medium was added (day –6). After additional 6 days (day 0), the cells were serum-starved to induce differentiation and assayed at day 3.

To deplete parental centrioles using centrinone (a gift from Dr. Karen Oegema, UCSD), the drug dissolved in DMSO was added to ependymal progenitors at day –7, together with the p53 inhibitor

pifithrin- α (10 μ M). The culture medium was changed every 2 days, with supplemented centrinone and pifithrin- α . We initially tested different concentrations (0.3, 0.75, 1.5, and 3 μ M) of centrinone and finally used 1.5 μ M as the optimal concentration. The cells were assayed at day 0 or day 3.

Experiments involving mouse tissues were performed in accordance with protocols approved by the Institutional Animal Care and Use Committee of Institute of Biochemistry and Cell Biology.

Plasmid constructs

The cDNAs of full-length mouse *Deup1* (NM_181816) and *Ccdc78* (NM_001165929) were PCR-amplified and subcloned into the lentiviral expression vector, pLV-GFP, to generate pLV-GFP-Deup1 and pLV-GFP-Ccdc78. To express GFP-Deup1 under the control of its own promoter, a 2-kb genomic DNA sequence of mouse *Deup1* upstream of the first exon was PCR-amplified and used to replace the CMV promoter of pLV-GFP-Deup1.

Antibodies

Secondary antibodies used for immunofluorescence (IF) were as follows: donkey anti-rabbit conjugated with Cy3 or DyLight 405, anti-chicken conjugated with Alexa Fluor-488 or DyLight-405, anti-mouse conjugated with Cy3 or DyLight-405, anti-rat conjugated with Alexa Fluor-488, anti-guinea pig conjugated with Cy3 (Jackson ImmunoResearch), and anti-mouse conjugated with Alexa Fluor-647 (Thermo Fisher Scientific). The DyLight 405-conjugated antibodies were used at 1:200, and the remaining antibodies were used at 1:1,000. Secondary antibodies used for Western blotting (WB) were HRP-conjugated goat anti-mouse and anti-rabbit antibodies (Thermo Fisher; 1:5,000).

Commercial primary antibodies used were as follows: mouse anti-Sas6 (sc-81431, Santa Cruz; IF 1:50), mouse anti-Centrin (04-1624(20H5), Millipore; IF 1:200), mouse anti- α -Tubulin (T5168, Sigma-Aldrich; WB 1:5,000), mouse anti-acetylated tubulin (T7451, Sigma-Aldrich; IF 1:1,000), mouse anti-Centrobilin (ab70448, Abcam; IF 1:200), mouse anti-Zo-1 (33-9100, Thermo Fisher; IF 1:1,000), rabbit anti-Centrin1 (12794-1-AP, Proteintech; IF 1:200), rat anti-GFP (sc-101536, Santa Cruz; IF 1:50), rabbit anti-GFP (A-11122, Thermo Fisher; WB 1:3,000), and rabbit anti-Cep63 (06-1292, Millipore; IF 1:200).

Rabbit anti-Deup1 (IF 1:200; WB 1:4,000), chicken anti-Cep152 (IF 1:300), and rabbit anti-Plk4 (IF 1:200; WB 1:2,000) antibodies were homemade [36]. To generate antibodies against murine Cep164, Odf2, or Ccdc78, cDNA fragments of mouse *Cep164* (NM_001081373; encoding 1–400 aa), *Odf2* (NM_001177659; encoding 401–826 aa), and *Ccdc78* (NM_001165929; encoding 1–437 aa) were PCR-amplified from the total cDNAs of mTECs. The cDNA fragments of *Cep164* and *Odf2* were subcloned into pET32a to express His-tagged fusion proteins. The cDNA of *Ccdc78* was subcloned into pGEX-4T-1 to express GST-fusion protein. The proteins were purified by using Ni-NTA beads (Qiagen) or glutathione-agarose beads (Sigma) and used as antigens. Rabbit anti-Cep164 (IF 1:200; WB 1:1,000), guinea pig anti-Odf2 (IF 1:200; WB 1:2,000), and rabbit anti-Ccdc78 (IF 1:200; WB 1:2,000) antibodies were generated through contracted services (ABclonal) and affinity-purified.

Immunofluorescent microscopy

Immunostaining and immunofluorescent microscopy were performed as described [36]. Briefly, mEPCs grown on glass-bottomed dishes and mTECs on Transwells were pre-extracted with 0.5% Triton X-100 in PBS for 40 s or for 3 min, respectively, followed by fixation with 4% fresh paraformaldehyde in PBS for 15 min at room temperature. After fixation, the cells were permeabilized with 0.5% Triton X-100 in PBS for 15 min and blocked with blocking buffer (4% BSA in TBST) for 1 h at room temperature. Primary and secondary antibodies were diluted into the blocking buffer and applied to cells at room temperature for 2 and 1 h, respectively, interspaced with three rounds of washing. The samples were imaged with a structured illumination microscope (GE OMX V3) with a 100 \times /1.40 NA oil-immersion objective lens (Olympus). Serial z-stack sectioning was performed at 125-nm intervals. Raw images were processed for maximum intensity projection with SoftWoRx software.

Confocal images were captured using Leica TCS SP8 system with a 63 \times /1.40 oil-immersion objective lens. Serial z-stack sectioning was set at 125-nm intervals. Images were processed with maximum intensity projections.

Live cell imaging

Mouse ependymal progenitors were infected with lentivirus at day -1 for the expression of GFP-Deup1 under *Deup1* promoter. Live cell imaging was performed at day 2.5. The images in Fig 3E, and Movies EV2 and EV3 were captured with an Olympus SpinSR10 spinning disk confocal super-resolution microscope equipped with an APON 60 \times OTIRF/1.49 NA oil objective (Olympus) and ORCA-Flash 4.0 V3 Digital CMOS Camera (Hamamatsu). The laser power (488 nm) was set to 10% to reduce cell toxicity. The images in Movie EV1 were recorded using an Andor Dragonfly high-speed confocal microscope equipped with a Plan Apo λ 60 \times /1.40 NA oil objective (Nikon) and a Zyla sCMOS camera (Andor). The laser power (488 nm) was set to 3%. The exposure time was 100 ms. The images were recorded at 5-min intervals for 12.5 h. z-stack sectioning was performed at 0.5- μ m intervals to cover a depth of 20 μ m. The images and movies were processed with Imaris (Bitplane) and ImageJ (Fiji) softwares.

Quantification and statistical analysis

Deuterosome diameters were measured from 3D-SIM images of Deup1 using the “automatic bright objects” mode of the “count/size” function of Image-Pro Plus 6.0 software (Media Cybernetics). Cells in different categories were scored manually using available original 3D-SIM images (1,024 \times 1,024 pixels), each of which contained multiple cells, from three independent experiments. Parental centrioles were identified and scored based on at least two different centriolar markers. Ciliary length of ependymal progenitors at day 0 and mEPCs at day 3 was measured using the “measurements” module of Image-Pro Plus 6.0. Quantification results are presented as mean \pm SD unless otherwise stated. Differences are considered significant when *P* was < 0.05 in a two-tailed unpaired Student's *t*-test using GraphPad Prism software (GraphPad Software).

Expanded View for this article is available online.

Acknowledgements

The authors thank Dr Nathalie Spassky (CNRS, France) for mEPC culture protocol, Dr. Karen Oegema (University of California, San Diego) for providing centriolone, the Centre for Biological Imaging (Institute of Biophysics, CAS) for support on 3D-SIM imaging, Dr. Wenjuan Cai and Kefeng Wang (Olympus Corporation) for support on spinning disk imaging, and Yanli Zhao (Bitplane) for support on Imaris. This work was supported by National Natural Science Foundation of China (31330045 to X.Z. and 31501092 to H.Z.), National Key R&D Program of China (2017YFA0503500), and Chinese Academy of Sciences (XDB19000000).

Author contributions

XZ and XY conceived and directed the project; HZ and QC performed major experiments; CF did the quantification of the ciliary length; QH generated the homemade antibodies; JZ provided the 3D-SIM imaging system; XZ, XY, and HZ designed experiments, interpreted data, and wrote the paper.

Conflict of interest

The authors declare that they have no conflict of interest.

References

- Banterle N, Gonczy P (2017) Centriole biogenesis: from identifying the characters to understanding the plot. *Annu Rev Cell Dev Biol* 33: 23–49
- Nigg EA, Holland AJ (2018) Once and only once: mechanisms of centriole duplication and their deregulation in disease. *Nat Rev Mol Cell Biol* 19: 297–312
- Nigg EA, Stearns T (2011) The centrosome cycle: centriole biogenesis, duplication and inherent asymmetries. *Nat Cell Biol* 13: 1154–1160
- Ito D, Bettencourt-Dias M (2018) Centrosome remodelling in evolution. *Cells* 7: 71
- Brown NJ, Marjanovic M, Luders J, Stracker TH, Costanzo V (2013) Cep63 and cep152 cooperate to ensure centriole duplication. *PLoS One* 8: e69986
- Sir JH, Barr AR, Nicholas AK, Carvalho OP, Khurshid M, Sossick A, Reichelt S, D'Santos C, Woods CG, Gergely F (2011) A primary microcephaly protein complex forms a ring around parental centrioles. *Nat Genet* 43: 1147–1153
- Kleylein-Sohn J, Westendorf J, Le Clech M, Habedanck R, Stierhof YD, Nigg EA (2007) Plk4-induced centriole biogenesis in human cells. *Dev Cell* 13: 190–202
- Bettencourt-Dias M, Rodrigues-Martins A, Carpenter L, Riparbelli M, Lehmann L, Gatt MK, Carmo N, Balloux F, Callaini G, Glover DM (2005) SAK/PLK4 is required for centriole duplication and flagella development. *Curr Biol* 15: 2199–2207
- Habedanck R, Stierhof YD, Wilkinson CJ, Nigg EA (2005) The Polo kinase Plk4 functions in centriole duplication. *Nat Cell Biol* 7: 1140–1146
- Hatch EM, Kulukian A, Holland AJ, Cleveland DW, Stearns T (2010) Cep152 interacts with Plk4 and is required for centriole duplication. *J Cell Biol* 191: 721–729
- Arquint C, Sonnen KF, Stierhof YD, Nigg EA (2012) Cell-cycle-regulated expression of STIL controls centriole number in human cells. *J Cell Sci* 125: 1342–1352
- Arquint C, Gabryjarczyk AM, Imseng S, Bohm R, Sauer E, Hiller S, Nigg EA, Maier T (2015) STIL binding to Polo-box 3 of PLK4 regulates centriole duplication. *Elife* 4: e07888
- Hilbert M, Noga A, Frey D, Hamel V, Guichard P, Kraatz SH, Pfreundschuh M, Hosner S, Fluckiger I, Jaussi R et al (2016) SAS-6 engineering reveals interdependence between cartwheel and microtubules in determining centriole architecture. *Nat Cell Biol* 18: 393–403
- Lane HA, Nigg EA (1996) Antibody microinjection reveals an essential role for human polo-like kinase 1 (Plk1) in the functional maturation of mitotic centrosomes. *J Cell Biol* 135: 1701–1713
- Loncarek J, Bettencourt-Dias M (2018) Building the right centriole for each cell type. *J Cell Biol* 217: 823–835
- Sonnen KF, Schermelleh L, Leonhardt H, Nigg EA (2012) 3D-structured illumination microscopy provides novel insight into architecture of human centrosomes. *Biol Open* 1: 965–976
- Moyer TC, Clutario KM, Lambrus BG, Daggubati V, Holland AJ (2015) Binding of STIL to Plk4 activates kinase activity to promote centriole assembly. *J Cell Biol* 209: 863–878
- Ohta M, Ashikawa T, Nozaki Y, Kozuka-Hata H, Goto H, Inagaki M, Oyama M, Kitagawa D (2014) Direct interaction of Plk4 with STIL ensures formation of a single procentriole per parental centriole. *Nat Commun* 5: 5267
- Pelletier L, O'Toole E, Schwager A, Hyman AA, Muller-Reichert T (2006) Centriole assembly in *Caenorhabditis elegans*. *Nature* 444: 619–623
- Kong D, Farmer V, Shukla A, James J, Gruskin R, Kiriya S, Loncarek J (2014) Centriole maturation requires regulated Plk1 activity during two consecutive cell cycles. *J Cell Biol* 206: 855–865
- Dzhindzhev NS, Yu QD, Weiskopf K, Tzolovsky G, Cunha-Ferreira I, Riparbelli M, Rodrigues-Martins A, Bettencourt-Dias M, Callaini G, Glover DM (2010) Asterless is a scaffold for the onset of centriole assembly. *Nature* 467: 714–718
- Strnad P, Leidel S, Vinogradova T, Euteneuer U, Khodjakov A, Gonczy P (2007) Regulated HsSAS-6 levels ensure formation of a single procentriole per centriole during the centrosome duplication cycle. *Dev Cell* 13: 203–213
- Vulprecht J, David A, Tibelius A, Castiel A, Konotop G, Liu F, Bestvater F, Raab MS, Zentgraf H, Izraeli S et al (2012) STIL is required for centriole duplication in human cells. *J Cell Sci* 125: 1353–1362
- Brooks ER, Wallingford JB (2014) Multiciliated cells. *Curr Biol* 24: R973–R982
- Ishikawa H, Marshall WF (2011) Ciliogenesis: building the cell's antenna. *Nat Rev Mol Cell Biol* 12: 222–234
- Spassky N, Meunier A (2017) The development and functions of multiciliated epithelia. *Nat Rev Mol Cell Biol* 18: 423–436
- Yan X, Zhao H, Zhu X (2016) Production of Basal Bodies in bulk for dense multicilia formation. *Fluorescence* 5: 1533
- Stubbs JL, Vladar EK, Axelrod JD, Kintner C (2012) Multicilin promotes centriole assembly and ciliogenesis during multiciliate cell differentiation. *Nat Cell Biol* 14: 140–147
- Ma L, Quigley I, Omran H, Kintner C (2014) Multicilin drives centriole biogenesis via E2f proteins. *Genes Dev* 28: 1461–1471
- Hoh RA, Stowe TR, Turk E, Stearns T (2012) Transcriptional program of ciliated epithelial cells reveals new cilium and centrosome components and links to human disease. *PLoS One* 7: e2166
- Kim S, Ma L, Shokhirev MN, Quigley I, Kintner C (2018) Multicilin and activated E2f4 induce multiciliated cell differentiation in primary fibroblasts. *Sci Rep* 8: 12369
- Mori M, Hazan R, Danielian PS, Mahoney JE, Li H, Lu J, Miller ES, Zhu X, Lees JA, Cardoso WV (2017) Cytoplasmic E2f4 forms organizing centres for initiation of centriole amplification during multiciliogenesis. *Nat Commun* 8: 15857
- Dirksen ER (1971) Centriole morphogenesis in developing ciliated epithelium of the mouse oviduct. *J Cell Biol* 51: 286–302

34. Sorokin SP (1968) Reconstructions of centriole formation and ciliogenesis in mammalian lungs. *J Cell Sci* 3: 207–230
35. Anderson RC, Brenner RM (1971) The formation of basal bodies (centrioles) in the Rhesus monkey oviduct. *J Cell Biol* 50: 10–34
36. Zhao H, Zhu L, Zhu Y, Cao J, Li S, Huang Q, Xu T, Huang X, Yan X, Zhu X (2013) The Cep63 paralogue Deup1 enables massive *de novo* centriole biogenesis for vertebrate multiciliogenesis. *Nat Cell Biol* 15: 1434–1444
37. Tang TK (2013) Centriole biogenesis in multiciliated cells. *Nat Cell Biol* 15: 1400–1402
38. Klos Dehring DA, Vladar EK, Werner ME, Mitchell JW, Hwang P, Mitchell BJ (2013) Deuterosome-mediated centriole biogenesis. *Dev Cell* 27: 103–112
39. Al Jord A, Shihavuddin A, Servignat d'Aout R, Faucourt M, Genovesio A, Karaiskou A, Sobczak-Thépot J, Spassky N, Meunier A (2017) Calibrated mitotic oscillator drives motile ciliogenesis. *Science* 358: 803–806
40. Revinski DR, Zaragosi LE, Boutin C, Ruiz-Garcia S, Deprez M, Thome V, Rosnet O, Gay AS, Mercey O, Paquet A et al (2018) CDC20B is required for deuterosome-mediated centriole production in multiciliated cells. *Nat Commun* 9: 4668
41. Beisson J, Wright M (2003) Basal body/centriole assembly and continuity. *Curr Opin Cell Biol* 15: 96–104
42. Kalnins VI, Porter KR (1969) Centriole replication during ciliogenesis in the chick tracheal epithelium. *Z Zellforsch Mikrosk Anat* 100: 1–30
43. Al Jord A, Lemaitre AI, Delgehr N, Faucourt M, Spassky N, Meunier A (2014) Centriole amplification by mother and daughter centrioles differs in multiciliated cells. *Nature* 516: 104–107
44. Meunier A, Spassky N (2016) Centriole continuity: out with the new, in with the old. *Curr Opin Cell Biol* 38: 60–67
45. You Y, Richer EJ, Huang T, Brody SL (2002) Growth and differentiation of mouse tracheal epithelial cells: selection of a proliferative population. *Am J Physiol Lung Cell Mol Physiol* 283: L1315–L1321
46. Vladar EK, Stearns T (2007) Molecular characterization of centriole assembly in ciliated epithelial cells. *J Cell Biol* 178: 31–42
47. Leidel S, Delattre M, Cerutti L, Baumer K, Gonczy P (2005) SAS-6 defines a protein family required for centrosome duplication in *C. elegans* and in human cells. *Nat Cell Biol* 7: 115–125
48. Nakazawa Y, Hiraki M, Kamiya R, Hirono M (2007) SAS-6 is a cartwheel protein that establishes the 9-fold symmetry of the centriole. *Curr Biol* 17: 2169–2174
49. Yang TT, Chong WM, Wang WJ, Mazo G, Tanos B, Chen Z, Tran TMN, Chen YD, Weng RR, Huang CE et al (2018) Super-resolution architecture of mammalian centriole distal appendages reveals distinct blade and matrix functional components. *Nat Commun* 9: 2023
50. Graser S, Stierhof YD, Lavoie SB, Gassner OS, Lamla S, Le Clech M, Nigg EA (2007) Cep164, a novel centriole appendage protein required for primary cilium formation. *J Cell Biol* 179: 321–330
51. Delgehr N, Meunier A, Faucourt M, Bosch Grau M, Strehl L, Janke C, Spassky N (2015) Ependymal cell differentiation, from monociliated to multiciliated cells. *Methods Cell Biol* 127: 19–35
52. Spassky N, Merkle FT, Flames N, Tramontin AD, Garcia-Verdugo JM, Alvarez-Buylla A (2005) Adult ependymal cells are postmitotic and are derived from radial glial cells during embryogenesis. *J Neurosci* 25: 10–18
53. Zheng J, Liu H, Zhu L, Chen Y, Zhao H, Zhang W, Li F, Xie L, Yan X, Zhu X (2019) Microtubule-bundling protein Spef1 enables mammalian ciliary central apparatus formation. *J Mol Cell Biol* 11: 67–77
54. Dammermann A, Merdes A (2002) Assembly of centrosomal proteins and microtubule organization depends on PCM-1. *J Cell Biol* 159: 255–266
55. Hori A, Peddie CJ, Collinson LM, Toda T (2015) Centriolar satellite- and hMsd1/SSX2IP-dependent microtubule anchoring is critical for centriole assembly. *Mol Biol Cell* 26: 2005–2019
56. Barlan K, Gelfand VI (2017) Microtubule-based transport and the distribution, tethering, and organization of organelles. *Cold Spring Harb Perspect Biol* 9: a025817
57. Stevenson BR, Siliciano JD, Mooseker MS, Goodenough DA (1986) Identification of ZO-1: a high molecular weight polypeptide associated with the tight junction (zonula occludens) in a variety of epithelia. *J Cell Biol* 103: 755–766
58. Lukinavicius G, Lavogina D, Orpinell M, Umezawa K, Reymond L, Garin N, Gonczy P, Johnsson K (2013) Selective chemical crosslinking reveals a Cep57-Cep63-Cep152 centrosomal complex. *Curr Biol* 23: 265–270
59. Martin CA, Ahmad I, Klingseisen A, Hussain MS, Bicknell LS, Leitch A, Nurnberg G, Toliat MR, Murray JE, Hunt D et al (2014) Mutations in PLK4, encoding a master regulator of centriole biogenesis, cause microcephaly, growth failure and retinopathy. *Nat Genet* 46: 1283–1292
60. Zou C, Li J, Bai Y, Gunning WT, Wazer DE, Band V, Gao Q (2005) Centrobin: a novel daughter centriole-associated protein that is required for centriole duplication. *J Cell Biol* 171: 437–445
61. Piperno G, Fuller MT (1985) Monoclonal antibodies specific for an acetylated form of alpha-tubulin recognize the antigen in cilia and flagella from a variety of organisms. *J Cell Biol* 101: 2085–2094
62. Wong YL, Anzola JV, Davis RL, Yoon M, Motamedi A, Kroll A, Seo CP, Hsia JE, Kim SK, Mitchell JW et al (2015) Cell biology. Reversible centriole depletion with an inhibitor of Polo-like kinase 4. *Science* 348: 1155–1160
63. Nanjundappa R, Kong D, Shim K, Stearns T, Brody S, Loncarek J, Mahjoub M (2018) Regulation of cilia abundance in multiciliated cells. *bioRxiv* <https://doi.org/10.1101/478297> [PREPRINT]
64. Mercey O, Al Jord A, Rostaing P, Mahuzier A, Fortoul A, Boudjema A, Faucourt M, Spassky N, Meunier A (2018) Dynamics of centriole amplification in centrosome-depleted brain multiciliated progenitors. *bioRxiv* <https://doi.org/10.1101/503730> [PREPRINT]
65. La Terra S, English CN, Hergert P, McEwen BF, Sluder G, Khodjakov A (2005) The *de novo* centriole assembly pathway in HeLa cells: cell cycle progression and centriole assembly/maturation. *J Cell Biol* 168: 713–722
66. Khodjakov A, Rieder CL, Sluder G, Cassels G, Sibon O, Wang CL (2002) *De novo* formation of centrosomes in vertebrate cells arrested during S phase. *J Cell Biol* 158: 1171–1181
67. Szollosi D, Ozil JP (1991) *De novo* formation of centrioles in parthenogenetically activated, diploidized rabbit embryos. *Biol Cell* 72: 61–66
68. Calarcogillam PD, Siebert MC, Hubble R, Mitchison T, Kirschner M (1983) Centrosome development in early mouse embryos as defined by an autoantibody against pericentriolar material. *Cell* 35: 621–629
69. Guirao B, Meunier A, Mortaud S, Aguilar A, Corsi JM, Strehl L, Hirota Y, Desoeuvre A, Boutin C, Han YG et al (2010) Coupling between hydrodynamic forces and planar cell polarity orients mammalian motile cilia. *Nat Cell Biol* 12: 341–350
70. Bazzi H, Anderson KV (2014) Acentriolar mitosis activates a p53-dependent apoptosis pathway in the mouse embryo. *Proc Natl Acad Sci USA* 111: E1491–E1500
71. Djuzenova CS, Fiedler V, Memmel S, Katzer A, Hartmann S, Krohne G, Zimmermann H, Scholz CJ, Polat B, Flentje M et al (2015) Actin cytoskeleton organization, cell surface modification and invasion rate of 5 glioblastoma cell lines differing in PTEN and p53 status. *Exp Cell Res* 330: 346–357